On the Nature of Memory and Rejuvenation in Glassy Systems

J. Freedberg,[1,*] W. Joe Meese,[1] J. He,[2] D. L. Schlagel,[3] E. Dan Dahlberg,[1] and R. L. Orbach[4]

[1] *School of Physics and Astronomy, The University of Minnesota, Minneapolis, Minnesota 55455, USA*
[2] *Department of Mechanical Engineering, The University of Texas at Austin, Austin, Texas 78712, USA*
[3] *Division of Materials Science and Engineering, Ames Laboratory, Ames, Iowa 50011, USA*
[4] *Texas Materials Institute, The University of Texas at Austin, Austin, Texas 78712, USA*

(Dated: May 17, 2023)

The memory effect in a single crystal spin glass ($Cu_{0.92}Mn_{0.08}$) has been measured using 1 Hz ac susceptibility measurements over a reduced temperature range of $0.4 - 0.7\,T_g$ and a model of the memory effect has been developed. A double-waiting-time protocol is carried out where the spin glass is first allowed to age at a temperature below T_g, T_{w_1}, followed by a second aging 4 K lower, T_{w_2}. The 4 K separation is sufficient to ensure rejuvenation has occurred. The model is based on calculating overlaps between the growth of the correlation lengths at the two temperatures. It accounts for the absolute magnitude of the memory effect as a function of both waiting times and temperatures. The data can be explained by the memory loss being a function of the relative change in the correlated volume at the first waiting temperature due to growth in the correlations at the second waiting temperature.

Introduction The origin and nature of memory and rejuvenation in spin glasses has been the subject of investigations, both experimental and theoretical, for over two decades [1–15]. When held at a temperature below the glass temperature T_g, the state of a spin glass is well known to age with time [16–18]. Rejuvenation is the process by which the spin glass appears to lose knowledge of its prior aging when the temperature is lowered. Memory, on the other hand, is displayed when the spin glass is reheated to the aging temperature and it recovers, at least partially, the aged state. Although there is some agreement to the origin of the aging phenomena [(JF) REFS], rejuvenation and memory present a conundrum that has eluded a satisfactory simultaneous explanation. The appearance of these effects together is central to understanding the spin glass state, in particular, how one can understand memory observed after rejuvenation.

This begs the question – if the spin glass appears to have "forgotten" it aged during rejuvenation, how can it "remember" its previous cooling history? Several explanations have been postulated, but never quantitatively tested experimentally [1, 11, 13, 19–21]. As we show in this letter, our double-waiting-time experiments and model explain this mystery.

In this letter, we use apparent spin glass memory loss in a single crystal of $Cu_{0.92}Mn_{0.08}$ as a probe of both memory and rejuvenation. Additionally, we present a simple physical model which correctly accounts for our results. We argue that this picture may provide an explanation for rejuvenation and memory in other glassy systems [22–24].

A canonical low frequency ac susceptibility measurement displaying the three out-of-equilibrium effects of aging, rejuvenation, and memory [1] is presented in Figure 1. The reference curve, where no aging is exhibited, is plotted alongside the curves that exhibit these three out-of-equilibrium effects. Traditionally [1, 20], and in our work, we focus on the imaginary part, χ'' of the susceptibility because the size of these effects is more pronounced than in the real part, χ'. We note that similar conclusions to the ones we present for χ'' can also be drawn for χ'.

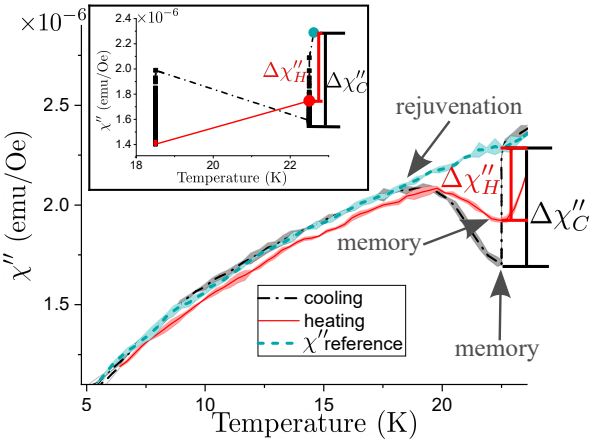

FIG. 1. The imaginary part of the 1 Hz magnetic susceptibility, $\chi''(\omega)$. The dashed data are the reference curve measured while continuously cooling the sample at 1 K/min. The dot-dash data include waiting at $T_{w_1} = 22.5$ K for a time $t_{w_1} = 1$ hour and the rejuvenation upon lowering the temperature; the temperature cooling rate is also 1 K/min. The solid curve is the heating data taken at a rate of 1 K/min that shows the memory effect back at T_{w_1}. The inset shows an example of a double-waiting-time experiment. $\Delta\chi''_C$ is the change in susceptibility during aging and $\Delta\chi''_H$ is the difference from the reference curve upon heating. For these data the cooling and heating rate is 35 K/min between the two waiting times.

Our efforts revolve around the following observation. As can be seen in Figure 1, while the heating curve (solid red line) does have knowledge of the cooling curve (black dot-dash line), they do not lie on top of each other. Importantly, this shows that spin glass memory

exhibits "memory loss." Of the many previous works that see memory, a few appear to see nearly perfect memory [1, 19], while others do not [11, 20]. A common qualitative picture states that memory is an effect of spin glass droplets whose dynamics are organized in a hierarchy ordered by their size. The distribution of droplet sizes correspond to a distribution of different relaxation times that are probed in spin glass experiments. However, recent simulation results [25] indicate that temperature chaos drives rejuvenation as a random process of destroying locally correlated regions of spin *overlap*, rather than just affecting the spin configurations themselves. These differing explanations again lead us to question how memory can *follow* rejuvenation, given that the system has gone chaotic and therefore lost knowledge of its previously grown correlated state.

Because of the recent progress made in understanding rejuvenation as a consequence of temperature chaos [25], we return to the observation of memory loss in spin glass. We follow the so-called "double memory" experiments by [11, 19], and focus on tuning the memory effect between two aging intervals at different temperatures separated by rapid temperature changes. In a similar spirit, we dub our protocols "double-waiting-time" experiments.

We quantify the memory, $\mathcal{M}$, by computing the ratio

$$\mathcal{M} \equiv \frac{\Delta\chi''_H}{\Delta\chi''_C} = \frac{\chi''_R(T_{w_1}) - \chi''(t_{w_1}+t_{w_2}, T_{w_1})}{\chi''_R(T_{w_1}) - \chi''(t_{w_1}, T_{w_1})}, \qquad (1)$$

shown pictorially in the inset of Figure 1. This quantity is a dimensionless parameter that compares the three measured susceptibilities. The numerator, $\Delta\chi''_H$, is the difference between the reference curve χ''_R at T_{w_1} and the susceptibility upon returning to T_{w_1} after having aged for an additional t_{w_2} at the lower temperature. The denominator, $\Delta\chi''_C$, is the difference between the reference curve χ''_R at T_{w_1} and the dynamic susceptibility at T_{w_1} after aging for t_{w_1}. Perfect memory occurs when $\chi''(t_{w_1}+t_{w_2}, T_{w_1}) = \chi''(t_{w_1}, T_{w_1})$ and corresponds to $\mathcal{M} = 1$. If there is no memory ($\mathcal{M}$= 0), the heating curve follows the reference curve, $\chi''(t_{w_1}+t_{w_2}, T_{w_1}) = \chi''_R(T_{w_1})$.

We shall ascribe rejuvenation to temperature chaos [26] recently observed experimentally [27] in a sample of $Cu_{0.92}Mn_{0.08}$ cut from the same boule as the sample we report on here. As shown computationally in Refs. [13, 25], when the temperature is lowered to T_{w_2} such that the spin glass has gone chaotic, then spin glass correlations develop over regions with a new length scale, with the relaxation occurring as if there were no correlations grown at T_{w_1}. Thus, we take the correlations at T_{w_1} and T_{w_2} to be independent. We have ensured our temperature drop of $T_{w_1} - T_{w_2} = 4\,\mathrm{K}$ is large enough to guarantee rejuvenation, as shown pictorially in Figure 1, has occurred in our double-waiting-time experiments.

From this argument, it follows that the memory effect is an interplay between correlation lengths, as recently confirmed [28]. In our experiments, we increase the correlation lengths by waiting for a variable amount of time. If we increase t_{w_1} while keeping t_{w_2} constant, then we would logically expect more memory at T_{w_1}. Alternatively, by holding t_{w_1} constant, but increasing t_{w_2}, then one would expect less memory at T_{w_1}. This argument is akin to the "temperature microscope" of Bouchaud *et al* [29] used to describe locally-ordered spin configurations within the droplet picture, as well as the phenomenological picture presented in Ref [11]. Importantly, the temperature microscope implies memory in the double-waiting-time experiments can be understood as a function of a single variable: the ratio between the dynamical correlation lengths grown at either temperature. Furthermore, other conventional pictures such as in Ref. [26] imply that **any** growth of **any** correlated regions at T_{w_2} will lead to memory loss. In what follows, we scrutinize this argument by measuring how the memory, defined in Eq. 1, varies throughout our double-waiting-time experiments.

Methods The following describes our undertaking of a systematic, quantitative study of the memory effect. All the ac susceptibility measurements were taken using a Magnetic Property Measuring System (MPMS) 3 [30] . The measurement frequency was 1 Hz, with an ac field amplitude of 10 Oe, sufficient to observe out-of-equilibrium effects while staying in the linear regime. For the reference susceptibility data shown in Figure 1, a cooling rate of 1 K/min was used. The glass temperature, T_g was found through dc magnetization measurements to be $T_g = 41.6$ K[31].

For the double-waiting-time experiments, we approximate a quench to be a cooling rate of 35 K/min to reduce unintended aging effects. For consistency in the measured results, the temperature was allowed to settle at each waiting temperature before recording the first measurement. While the temperature change from T_{w_1} to T_{w_2} is only about 10 seconds, the first data point taken was around 100 seconds. For each recorded point, 10 measurements were averaged. We opted to use the cooling protocol pictured in the inset of Figure 1. The protocol for our double-waiting-time experiments was as follows. First, the system was quenched from $T = 60\,\mathrm{K} > T_g$ to an aging temperature $T_{w_1} < T_g$ and is allowed to relax for a time t_{w_1}. Then, the system was quenched to a lower temperature $T_{w_2} < T_{w_1}$ where it evolved for time t_{w_2}. Finally, the system was then rapidly heated to the starting temperature T_{w_1} where the susceptibility was compared to the reference system. The temperature drop $\Delta T = T_{w_1} - T_{w_2}$ was chosen to ensure that the sample has fully rejuvenated; this ΔT is held fixed at 4 K.

Results and Discussion In Figure 2, we see that the double-waiting-time protocol can have a significant effect

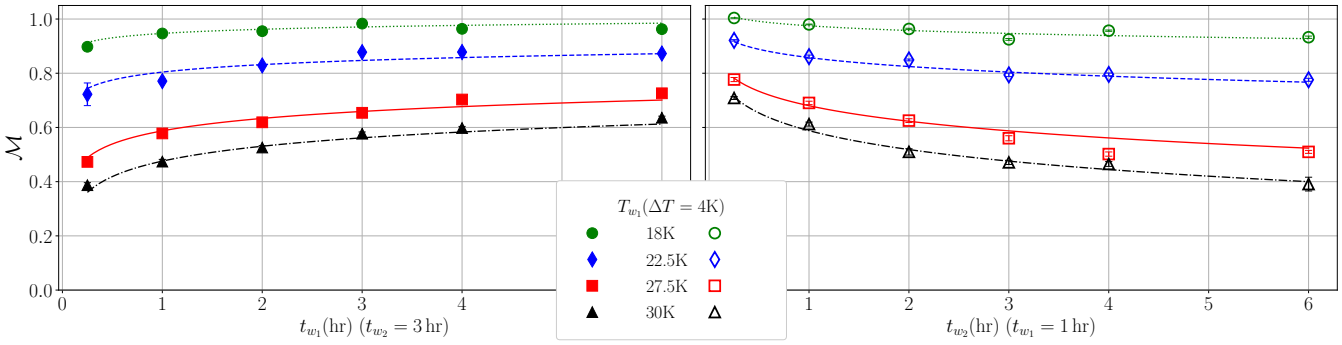

FIG. 2. For both a. and b., the first and second waiting temperatures are the same: T_{w_1} (18, 22.5, 27.5, and 30 K) and $T_{w_1} - T_{w_2} = 4\,\text{K}$. In both cases either the first (a.) or second (b.) waiting times were varied from $0 - 6$ hours (the horizontal axis), while the other waiting time was fixed at 3 and 1 hour, respectively. Closed markers indicate a variation of the first waiting time, while Open markers indicate a variation of the second waiting time. The lines are predictions based our model. The statistical error bars are present on each data point, though they are typically smaller than the marker.

on the magnitude of the memory retained. The trend is clear – the longer t_{w_1}, the more memory is retained, but the longer t_{w_2}, the less memory is retained. Additionally, in experiments with a lower set of waiting temperatures, more memory is always retained than in ones that have a higher set of waiting temperatures. Furthermore, the fact that the memory coefficient *increases* with t_{w_1} means that the memory loss seen is more complicated than the picture presented in Ref. [26] where any growth in the correlation length leads to memory loss. Indeed, this increase suggests that the degree to which temperature chaos erases the spin glass' memory is a gradual, rather than an abrupt, process.

There are at least two length scales at play – the size of correlations at T_{w_1}, and those at T_{w_2}. We estimate the correlation length based on the relationship developed by Kisker and Rieger [32]

$$\frac{\xi(t,T)}{a_0} = c_1 \left(\frac{t}{\tau_0}\right)^{c_2 T/T_g}, \tag{2}$$

where a_0 is the average spacing between manganese impurities, $\tau_0 \approx 2 \times 10^{-13}$, the timescale of microscopic fluctuations, $c_1 \approx 1$ and $c_2 \approx 0.1$. These estimates have been compared to three experimentally extracted correlation lengths (starred points) using a dc protocol.

The data in Figure 2 can be described by the temperature microscope picture, which considers the ratio of the correlation length ξ_2 at T_{w_2} to ξ_1 at T_{w_1}. In this picture, an increase in ξ_1 leads to a decrease in ξ_2/ξ_1, and an increase in ξ_2 leads to an increase in ξ_2/ξ_1, exactly what is seen in Figure 2, and it is consistent with the qualitative pictures discussed in the literature [11, 29].

This analysis with only two length scales implicitly makes another prediction, however. Considering that memory is a dimensionless quantity, and that it clearly depends on both length scales, one would expect that memory would be a function only of their ratio, ξ_2/ξ_1, if these are the only length scales relevant in the experiment. Therefore, double-waiting-time experiments that hold this ratio constant would always exhibit constant memory. We tested this prediction using the expressions for the dynamical correlation lengths in Equation 2, by identifying multiple experiments from Figure 2 that hold the calculated ratio ξ_2/ξ_1 fixed. We show these results in Figure 3. As seen in this figure, for three different constant values of ξ_2/ξ_1, memory is not constant. In fact, not only does the memory vary, it *decreases* with increasing ξ_1, seemingly counter to the results in Figure 2a where memory increases with increasing ξ_1. It is evident then that the specific details of the protocol dictate whether an increase in ξ_1 increases or decreases $\mathcal{M}$. Thus, memory must explicitly depend on ξ_1. However, since memory by definition is dimensionless, there must be at least one other independent length scale which also controls $\mathcal{M}$.

To understand these results, we have developed a model whose derivation is given in the supplemental materials. We consider a growing correlated region of size ξ_1 at waiting temperature T_{w_1}, encapsulated by a volume $V_\ell = \ell\ell_\perp^2$. Here, we take ℓ and $\ell_\perp$ length scales that are parallel and perpendicular to the ac field, and we require that they are large enough to consider different volumes of size V_ℓ as statistically independent. In equilibrium, and in the absence of a real-space anisotropy, we would expect that these scales are both equal to a static, isotropic correlation length. For the sake of generality in modeling the (dynamical) experimental data, we make the *ansatz* that they are different from each other.

The spin glass state evolves as the dynamical correlation length ξ grows. Now, consider a quench to T_{w_2}. Since we have cooled to a sufficiently low temperature such that the sample has fully rejuvenated, the spin glass energy landscape at T_{w_2} does not have the same set of minima as it does at T_{w_1}. This means that any new correlations at T_{w_2} grow independently from those at T_{w_1}.

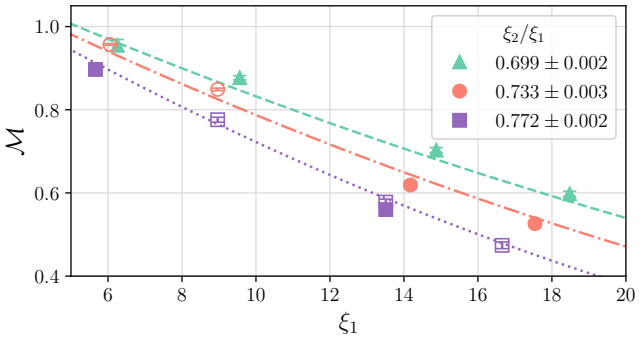

FIG. 3. $\mathcal{M}$ plotted as a function of ξ_1 for three different values of fixed ξ_2/ξ_1. Since the memory can be decreased by either increasing or decreasing ξ_1 depending on the conditions of the experiment, this strongly indicates the presence of another length scale. The solid lines are the fits to the data using the model presented in this letter. Statistical error bars are present on each data point, though they are typically smaller than the marker.

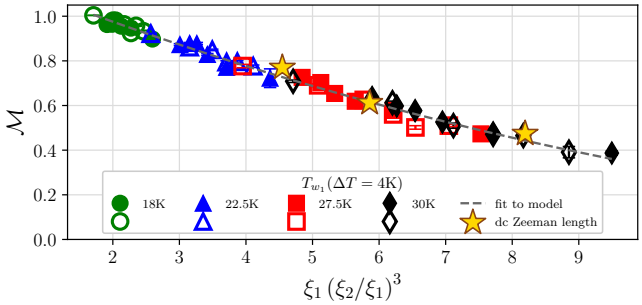

FIG. 4. The data from Figure 2 plotted against the model presented in Equation 4. Additionally, the three starred data points use correlation lengths were extracted from dc experiments with the ac values of memory. The data collapse supports our model. T_{w_1} (18, 22.5, 27.5, and 30 K) and $T_{w_1} - T_{w_2} = 4\,\text{K}$. In both cases either the first (closed markers) or second (open markers) waiting times are varied from $0-6$ hours, while the other waiting time is fixed at 3 and 1 hour, respectively. Statistical error bars are present on each data point, though they are typically smaller than the marker.

This is consistent with the probabilistic nature of temperature chaos that has been found numerically [25]. From there, we can model this as a single correlated region of volume V_{ξ_1} growing within V_ℓ, only then to have secondary correlated regions of volume V_{ξ_2} growing independently from the first. Thus, upon quenching to T_{w_2}, the new regions can appear anywhere within V_ℓ with an assumed uniform probability. If any new growth at T_{w_2} overlaps with the original cluster during the waiting time t_{w_2}, then we assume this reduces the memory upon returning to T_{w_1}.

Within this model, memory loss is the average relative change in V_{ξ_1} within V_ℓ after randomly developing new clusters at T_{w_2}. That is to say we must compute $\overline{\Delta V}/V_{\xi_1}$, where the overbar denotes statistical averaging over all independent volumes of size V_ℓ. Details of how we calculated $\overline{\Delta V}/V_{\xi_1}$ can be found in the supplemental material, but the main point is that the average change in volume $\overline{\Delta V}$ depends on where V_{ξ_2} grows – within, at the edge of, or outside V_{ξ_1}. The final expression for a spherical correlated volume, $\overline{\Delta V}/V_{\xi_1}$, is proportional to

$$\frac{\overline{\Delta V}}{V_{\xi_1}} \propto \frac{V_{\xi_1}}{V_\ell}\left(\frac{\xi_2}{\xi_1}\right)^3. \tag{3}$$

From this expression, and by comparing it with Figure 3, we identify two cases that help ascertain the behaviors of ℓ and $\ell_\perp$ from our *ansatz*. The first case would be if there is no independent length scale at the first waiting temperature other than ξ_1, thereby implying $\ell \sim \xi_1$ and $\ell_\perp \sim \xi_1$. Thus, Equation 3 would predict that memory loss only depends of the dimensionless ratio ξ_2/ξ_1, incompatible with the data shown in Figure 3. The second case, meanwhile, would be that there is spatial isotropy, $\ell = \ell_\perp$, but they are independent of ξ_1. In this case, Equation 3 would imply that memory loss does not depend on ξ_1 at all, again incompatible with the experimental results. Hence, we conclude only one length scale must indeed scale with ξ_1 while the other is independent of it. The only anisotropy in the problem that we can identify is due to the external ac field (albeit in spin-space rather than real-space), and therefore we take $\ell_\perp \sim \xi_1$ and ℓ to be the independent length scale. By substitution into Equation 3, we have

$$\frac{\overline{\Delta V}}{V_{\xi_1}} \propto \frac{4\pi}{3}\frac{\xi_1}{\ell}\left(\frac{\xi_2}{\xi_1}\right)^3. \tag{4}$$

With this expression, we combine all data from Figure 2 into a single plot shown in Figure 4, with the measured memory being the vertical axis and the calculated value of $\xi_1(\xi_2/\xi_1)^3$ being the horizontal. We see clear evidence of data collapse from all of the double-waiting-time experiments, indicating that the memory effect in these experiments are not functions of only the ratio ξ_2/ξ_1, as expected from previous work [11, 13, 20], but rather memory depends on *both* length scales explicitly. Indeed, as our model suggests, the only way the dimensionless quantity of memory can be a function of both lengths is if there is at least another length scale present: ℓ. From our model, we can provide an interpretation for this length. Its size, compared to ξ_1, controls how probable it is for new correlated regions grown at the second waiting temperature to overlap with those from the first waiting temperature. For it is only growth at T_{w_2} that overlaps with the original growth at T_{w_1}, rather than any growth at all, that leads to memory loss.

We wish to emphasize that the data shown in Figure 4 comes from 48 independent double-waiting-time experiments, and the horizontal axis represents a protocol-dependent, calculated value from Equation 4. The fact

that this shows a distinct data collapse represents agreement between these independent trials and provides strong evidence supporting the mechanism of memory loss outlined above. Random competition between the growth of correlated volumes at the two waiting temperatures drives memory loss in spin glass, with a separate length scale controlling the strength of the memory loss.

Now, the data shown in Figure 3 can be understood as well. If the ratio ξ_2/ξ_1 is fixed, any increase in ξ_1 will lead to an increase in memory loss by Equation 4, and therefore a corresponding decrease in $\mathcal{M}$. This is to be contrast with Figure 2a, where increasing ξ_1 with fixed ξ_2 will lead to a decrease in the term $\xi_1 \left(\xi_2/\xi_1\right)^3$, thereby increasing memory.

It is possible to be more precise with our modeling. As shown in the supplemental materials, since the reduction in χ'' corresponds to an increase in ξ, the relation between $\mathcal{M}$ and $\overline{\Delta V}/V_{\xi_1}$ is predicted to be of the form

$$\mathcal{M} = w\left[1 - \frac{4\pi}{3}\frac{\xi_1}{\ell}\left(\frac{\xi_2}{\xi_1}\right)^3\right]^{p/d}, \tag{5}$$

where $w \sim \mathrm{O}(1)$, ℓ, and p are unknown fitting parameters. For Figure 4, the values of w, ℓ, and p are found to be [(JM) change w_2 to ℓ with error and units (a_0)]$w = 1.2 \pm 0.02$, $w_2 = 0.04 \pm 0.01$, and $p = 7.11 \pm 2.1$ and $d = 3$, the spatial dimension.

This predicted fit is shown in Figure 4, and we find that the data in Figures 2 and 3 are well-represented by this model. Notably, the same three fitting parameters are used for all eight curves in Figure 2 and the three constant ξ_2/ξ_1 curves in Figure 3.

Conclusions Using quantitative measures of memory loss in spin glass systems, we have developed a model that explains memory. We find that overlapping, independent growth of spin glass correlations in double-waiting-time experiments controls the memory loss we observe. By modeling the amount of memory retained as a function of dynamical correlation length growth, we find that there exists an additional spatial length scale that controls the impact the independent growth of correlations from the second waiting temperature has on established correlated regions grown at the first waiting temperature.

Our modeling relies on it being possible to separate the spin glass sample into uncorrelated anisotropic volumes of size $V_\ell = \ell\ell_\perp^2$, spanned by two length scales ℓ and $\ell_\perp$. Fitting our model to our data requires that the latter, $\ell_\perp$, measured in the plane normal to the ac field, scales with the dynamical correlation length grown at the first waiting temperature, $\xi_1(t_{w_1}, T_{w_1})$, whereas the former, ℓ, is independent of it. This implies that a spatial anisotropy exists in the problem that, at this point, is not understood. There are several mechanisms that can yield a *spin-space* anisotropy in spin glasses – such as an external magnetic field acting as an effective uniaxial random field [33], or magnetic anisotropies which may induce chiral ordering in vector spin glasses [34]. While these spin-space anisotropies may be present in our sample, it remains unclear why these spin-space effects would impact the real-space growth of spin glass correlations in a cubic crystal like CuMn. Despite this, the data collapse in Figure 4 is consistent with there being an independent length scale controlling memory, and our model suggests that this scale is spatially anisotropic. It is possible that this anisotropy is a dynamical effect that would presumably decay away in equilibrium (if they spin glass samples could relax long enough to reach it), or it may indicate that crystalline defects, such as dislocations, play a role in spin glass dynamics in an analogous way to what is seen in other disordered magnetic systems [35–39].

At the same time, our results open new and exciting lines of inquiry. For example, it has been noted [1] that these out-of-equilibrium measurements must be taken at very low frequencies, otherwise, aging vanishes. This means that the measuring frequency must introduce another time or length scale into this problem – but how it exactly does so is unclear.

It is important to emphasize that the spin glass correlated volumes as described in this letter are not just due spin-spin correlations as suggested in the droplet picture [40]. Instead, given the recent numerical results on temperature chaos driven rejuvenation [25], these correlated volumes are grown in the local Edwards-Anderson overlap. Crucially, this allows a description of memory following rejuvenation – when the temperature is lowered, it is the overlap, rather than the spin configurations which are frozen in, or "imprinted". Once the system goes chaotic, the growth of correlations at either waiting temperature will be independent of the growth of correlations at the other waiting temperature. However, the correlations at the lower temperature could form in the same location as the original correlated regions. When this occurs, the volume of the original correlated region decreases, leading to the memory loss observed. It is anticipated that this picture can shed light on other glassy systems which exhibit rejuvenation and memory [(JF) REFS].

Acknowledgements The authors wish to thank the Janus II group, and especially Ilaria Paga, Victor Martin-Mayor, Juan Ruiz-Lorenzo, and Enzo Marinari for their collaboration. Additionally, we thank Virginia Gali for a careful reading of the manuscript, as well as Kan-Ting Tsai and Gregory G. Kenning for helpful discussions. This work was supported by the U.S. Department of Energy, Office of Basic Energy Sciences, Division of Materials Science and Engineering, under Award No. DE-SC0013599. All experiments were carried out at the Institute for Rock Magnetism (IRM) at the University of Minnesota which is supported by the National Science Foundation, Division of Earth Sciences, Instrumentation and Facilities under Award No. 2153786. The authors wish to thank Peat Solheid, Maxwell Brown, Dario Bilardello, Joshua Feinberg, and Bruce Moskowitz from the

IRM for much equipment time, training, and access to this instrument.

* freed114@umn.edu

[1] K. Jonason, E. Vincent, J. Hammann, J. P. Bouchaud, and P. Nordblad, Phys. Rev. Lett. **81**, 3243 (1998).

[2] E. Vincent, in *Ageing and the Glass Transition*, Lecture Notes in Physics No. 716, edited by M. Henkel, M. Pleimling, and R. Sanctuary (Springer, 2007).

[3] V. Dupuis, F. Bert, J.-P. Bouchaud, J. Hammann, F. Ladieu, D. Parker, and E. Vincent, Pramana J. of Phys. **64**, 1109 (2005).

[4] L. Berthier and J.-P. Bouchaud, Phys. Rev. B **66**, 054404 (2002).

[5] E. Vincent, J. Hammann, M. Ocio, J.-P. Bouchaud, and L. F. Cugliandolo, in *Complex Behavior of Glassy Systems*, Lecture Notes in Physics No. 492, edited by M. Rubí and C. Pérez-Vicente (Springer, 1997).

[6] J. Hammann, E. Vincent, V. Dupuis, M. Alba, M. Ocio, and J.-P. Bouchaud, J. Phys. Soc. Jpn. , Suppl A. 206 (2000).

[7] L. Berthier and A. P. Young, Phys. Rev. B **71**, 214429 (2005).

[8] E. Vincent, J. P. Bouchaud, D. S. Dean, and J. Hammann, Phys. Rev. B **52**, 1050 (1995).

[9] Refregier, Ph., Vincent, E., Hammann, J., and Ocio, M., J. Phys. France **48**, 1533–1539 (1987).

[10] E. Vincent, J. P. Bouchaud, J. Hammann, and F. Lefloch, Philosophical Magazine B **71**, 489–500 (1995), https://doi.org/10.1080/01418639508238540.

[11] K. Jonason, P. Nordblad, E. Vincent, J. Hammann, and J.-P. Bouchaud, Eur. Phys. J. B **13**, 99 (2000).

[12] M. Sasaki, V. Dupuis, J.-P. Bouchaud, and E. Vincent, Eur. Phys. J. B **29**, 469 (2002).

[13] S. Miyashita and E. Vincent, Eur. Phys. J. B **22**, 203 (2001).

[14] H. Yoshino, A. Lemaıtre, and J.-P. Bouchaud, Eur. Phys. J. B **20**, 367 (2001).

[15] P. E. Jönsson, R. Mathieu, P. Nordblad, H. Yoshino, H. A. Katori, and A. Ito, Phys. Rev. B **70**, 174402 (2004).

[16] L. Lundgren, P. Svedlindh, and O. Beckman, J. Magn. Magn. Mater. **31–34**, 1349 (1983).

[17] R. V. Chamberlin, Physical Review B **30**, 5393 (1984).

[18] M. Ocio, M. Alba, and J. Hammann, Journal de Physique Lettres **46**, 1101 (1985).

[19] F. Lefloch, J. Hammann, M. Ocio, and E. Vincent, EPL (Europhysics Letters) **18**, 647 (1992).

[20] T. Jonsson, K. Jonason, P. Jönsson, and P. Nordblad, Phys. Rev. B **59**, 8770 (1999).

[21] E. Vincent, V. Depuis, M. Alba, J. Hammann, and J.-P. Bouchaud, Europhys. Lett. **50**, 674 (2000).

[22] Y. Chen, Q. Zhang, S. Ramakrishnan, and R. L. Leheny, The Journal of Chemical Physics **158**, 024906 (2023), https://doi.org/10.1063/5.0126432.

[23] R. Kürsten, V. Sushkov, and T. Ihle, Phys. Rev. Lett. **119**, 188001 (2017).

[24] A. Prados and E. Trizac, Phys. Rev. Lett. **112**, 198001 (2014).

[25] M. Baity-Jesi, E. Calore, A. Cruz, L. A. Fernandez, J. M. Gil-Narvion, I. Gonzalez-Adalid Pemartin, A. Gordillo-Guerrero, D. Iñiguez, A. Maiorano, E. Marinari, V. Martin-Mayor, J. Moreno-Gordo, A. Muñoz Sudupe, D. Navarro, I. Paga, G. Parisi, S. Perez-Gaviro, F. Ricci-Tersenghi, J. J. Ruiz-Lorenzo, S. F. Schifano, B. Seoane, A. Tarancon, R. Tripiccione, and D. Yllanes, Communications physics **4**, 74 (2021), https://www.nature.com/articles/s42005-021-00565-9.pdf.

[26] A. J. Bray and M. A. Moore, Phys. Rev. Lett. **41**, 1068 (1978).

[27] Q. Zhai, R. L. Orbach, and D. L. Schlagel, Phys. Rev. B **105**, 014434 (2022).

[28] M. Baity-Jesi, E. Calore, A. Cruz, L. A. Fernandez, J. M. Gil-Narvion, I. Gonzalez-Adalid Pemartin, A. Gordillo-Guerrero, D. Iñiguez, A. Maiorano, E. Marinari, V. Martin-Mayor, J. Moreno-Gordo, A. Muñoz Sudupe, D. Navarro, I. Paga, G. Parisi, S. Perez-Gaviro, F. Ricci-Tersenghi, J. J. Ruiz-Lorenzo, S. F. Schifano, B. Seoane, A. Tarancon, and D. Yllanes, arXiv:2207.06207 (2023), Nature Physics (in press).

[29] J.-P. Bouchaud, V. Dupuis, J. Hammann, and E. Vincent, Phys. Rev. B **65**, 024439 (2001).

[30] Quantum Design North America, 10307 Pacific Center Court San Diego, CA 92121.

[31] The exact value is determined when the field cooled and zero field cooled curves diverge, known as the "onset of irreversibility".

[32] H. Rieger, J. Phys. A **26**, L615 (1993).

[33] A. Aharony, Phys. Rev. B **18**, 3328 (1978).

[34] H. Kawamura, Phys. Rev. Lett. **68**, 3785 (1992).

[35] D. Boyanovsky and J. L. Cardy, Phys. Rev. B **26**, 154 (1982).

[36] V. V. Prudnikov, Journal of Physics C: Solid State Physics **16**, 3685 (1983).

[37] I. D. Lawrie and V. V. Prudnikov, Journal of Physics C: Solid State Physics **17**, 1655 (1984).

[38] V. Blavats'ka, M. Dudka, R. Folk, and Y. Holovatch, Phys. Rev. B **72**, 064417 (2005).

[39] O. Vasilyev, B. Berche, M. Dudka, and Y. Holovatch, Phys. Rev. E **92**, 042118 (2015).

[40] D. S. Fisher and D. A. Huse, Phys. Rev. B **38**, 373 (1988).